

Time evolution of β -lactoglobulin corona formation on gold nanoparticles and impact on allergy

Xiaoning Zhang (✉ xiaoningzhang@126.com)

Qilu University of Technology <https://orcid.org/0000-0002-5914-5437>

Meifeng Li

Chengdu University of Traditional Chinese Medicine

Yuanping Lv

Sichuan University

Xiaoling Sun

Qilu University of Technology

Yao Han

Qilu University of Technology

Xiangzhong Zhao

Qilu University of Technology

Xiaowen Huang

Qilu University of Technology

Research

Keywords: Gold nanoparticles (AuNPs), β -lactoglobulin (β lg), protein corona, Au-S bonds, desensitization

Posted Date: February 11th, 2020

DOI: <https://doi.org/10.21203/rs.2.23072/v1>

License:  This work is licensed under a Creative Commons Attribution 4.0 International License.

[Read Full License](#)

Time evolution of β -lactoglobulin corona formation on gold nanoparticles and impact on allergy

Xiaoning Zhang^{1,*}, Meifeng Li², Yuanping Lv³, Xiaoling Sun¹, Yao Han¹, Xiangzhong Zhao^{1,*} and Xiaowen Huang^{4,*}

***Correspondence:** xiaoningzhang@126.com (X. Zhang); xiangzhongzhao@126.com (X. Zhao); huangxiaowen2013@gmail.com (X. Huang)

Abstract: Gold nanoparticles (AuNPs) are modified immediately by the adsorption of β -lactoglobulin (β lg) when designed as colorimetric probe in raw milk, leading to the formation of a protein corona. This adsorption results mainly from a fast electrostatic force and a slow formation of Au-S covalent bonds, which is a precondition for the use of AuNPs in biodetection. The proteins corona influences the structure and bioactivity of adsorbed protein, such as the allergy. In this study, the mechanism of β lg adsorbed on AuNPs was investigated in terms of stoichiometry, binding affinity (K_a), time evolution of Au-S bond, and general secondary structure changes to address the desensitization of AuNPs. The results show that about 3,600 β lg are adsorbed on a single AuNPs, and the K_a is $2.9 \pm 0.7 \times 10^6 \text{ M}^{-1}$. The formation of Au-S bonds takes about 9 h, which is the time needed for complete changes in secondary structure and the IgE combining capacity. The structure of allergenic epitopes assigned to β -sheet was destroyed by the formation of Au-S bond, then induced to the decrease allergy. Furthermore, Fourier transform infrared spectroscopy confirmed a decrease in β -sheet contents after conjugated with AuNPs.

Keywords: Gold nanoparticles (AuNPs), β -lactoglobulin (β lg), protein corona, Au-S bonds, desensitization

1. Introduction

Gold nanoparticles (AuNPs) have been known a significantly developments in the field of biotechnology and biomedicine [1-6], as sensing probes [2,3] and in drug delivery [4,5] and cancer therapy areas [6], because of their high surface energy and unique chemical and optical properties [3,6]. Especially in biodetection, AuNPs are commonly designed as a sensitive colorimetric probe in raw milk to detect of

melamine, tetracycline and tobramycin [7,8]. However, nanoparticles (NPs) surface is modified directly by the adsorption of proteins, forming a “protein corona” when exposed to the biological matrix (ie, milk) as a colorimetric probe [3,9,10], which consists of a hard corona or soft corona with strong or weak binding force, respectively, to the NPs surface [9,11]. The formation of a protein corona is a double-edged sword in biodetection [12], On one hand, it would improve the utilization and intracellular fate of AuNPs, especially those that enter into the organism [13], on the other hand, it not only hinders the efficiency of detection [14], but also may change the conformation of proteins and further perturbs their normal function and activity [15,16]. However, from this perspective of denaturing proteins, this adverse property can be extended to denature the unwanted or harmful proteins, such as allergenic proteins in milk.

Allergic reactions to food are causing increasing concern around the world, especially of milk allergy, which is one of the most common and serious of the immediate hypersensitivity reactions to food in terms of persistence and severity of reaction [17,18]. β -lactoglobulin (β lg) is one of the main allergenic proteins that contribute to milk allergies [19], and it contains of 162 amino acids residues with a molecular mass of 18.4 kDa. There are five cysteine residues with four involved in two disulfide bridges (Cys66-Cys160 and Cys106-Cys119) and one free thiol group (Cys121) [20]. β lg can be mediated by allergen-specific immunoglobulin E (IgE) antibodies that causes mast cell receptors to crosslink, inducing a signal transduction cascade that ends in degranulation and release of a variety of mediators [21]. Desensitization is a complex but a necessary process for the food safety. Nowadays, Heating and hydrolyzing are the most common treatments to decrease IgE binding and hypersensitivity of milk by changing the structural and chemical properties of β lg. Whereas, high temperature treatments (Maillard reaction or glycation) would decrease the biological properties and nutrition of the food, hydrolyzation could expose some inner epitopes to induce another allergen in some case [19,22,23]. Thus, developing better desensitization methods will be of great potential importance in food safety.

NPs-denatured adsorbed proteins provide a new approach for the desensitization, and a deep and comprehensive understanding of binding mechanism of β lg and AuNPs is required when it used as the desensitizer to food allergy. Adsorption of proteins upon the NPs surface is a complex dynamic process and depends on several factors, such as the size, charge and material of the NPs, as well as which protein it interacts with (number of cysteine residues) [11]. Moreover, binding affinity (K_a) and stoichiometry (molar ratio) are the critical parameters describing the adsorption.³ It is conceivable that β lg would be adsorbed on the surface of AuNPs to form a β lg corona (AuNPs- β lg conjugates) through a fast electrostatic force (ionic interactions and hydrogen bonds), as well as a slow formation of Au-S covalent bond [24]. The Au-S covalent bond is identified as the main force to induce the structural and conformational changes of proteins, and determine their stability and functional properties.¹⁴ This corona of native-like or unfolded proteins expressed at the surface of the AuNPs is the key phenomenon for the desensitization of NPs [25,26].

In the present work, we implemented a range of methods for studying binding mechanism of β lg-AuNPs interactions that facilitated a deeper understanding of NPs applied in the field of desensitization. In particular, transmission electron microscopy (TEM) was used to observe the corona image and details. Dynamic light scattering (DLS) was used to detect the hydrodynamic diameter changes of AuNPs before and after incubation with β lg, as well as the molar ratio. Isothermal titration calorimetry (ITC) and fluorescence quenching (FQ) were used to determine adsorbed parameters, such as, the K_a , binding sites of AuNPs and β lg, respectively. Surface enhanced raman spectrum (SERS) was used to illustrate the adsorbed mechanism of β lg and AuNPs that the time of the Au-S bond up-shifted. Fourier transform infrared spectroscopy (FTIR) was used to monitor the complete secondary structure changes of β lg and the relation with the formation of Au-S bonds. Finally, An indirect enzyme-linked immunosorbent assay (ELISA) and inhibition ELISA was performed to determine the changes of IgE combining capacity to evaluate the allergy of AuNPs- β lg conjugates at different incubation time. Figure 1 illustrates the schematic

overview of β lg adsorbed on the surface AuNPs by Au-S covalent bonds and decreased IgE combining capacity and allergy.

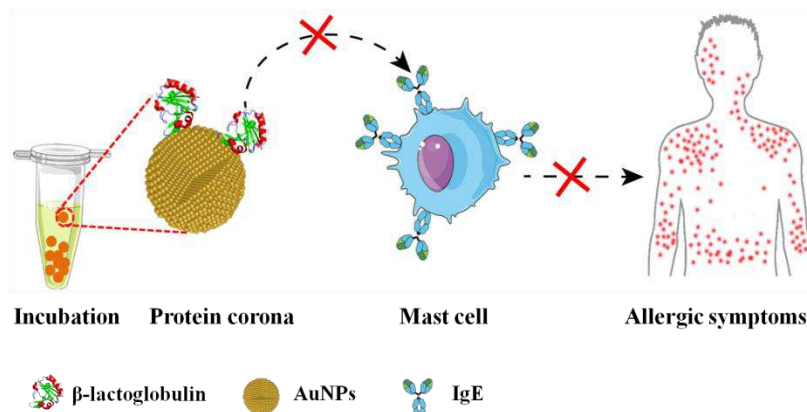


Figure 1. Scheme of β lg adsorbed on the surface of AuNPs by Au-S bonds and denaturation of IgE combining capacity and allergy.

2. Materials and methods

2.1. Materials. Bovine β -lactoglobulin (β lg) from bovine milk, goat antihuman IgE-HRP, and tetrachloroaurate ($\text{HAuCl}_4 \cdot 3\text{H}_2\text{O}$) were purchased from Sigma Aldrich (USA). Other chemical reagents were of analytical grade and were purchased from Sinopharm Chemical Reagents Co., Ltd. (Shanghai, China).

2.2. Fabrication of AuNPs. AuNPs were fabricated by chloroauric acid reduced by sodium citrate [27]. Briefly, 100 ml HAuCl_4 ($10^{-2}\%$, w/v) was reduced by 1 ml sodium citrate (1%, w/v) to fabricate ~ 40 nm AuNPs using vigorous stirring under boiling for 30 min. The resulting suspension was cooled to room temperature under continuous stirring then stored at 4°C in the dark. The concentration was calculated using the UV-vis method [28].

2.3. Transmission electron microscopy. AuNP- β lg conjugates were obtained by incubating β lg (200 μl , 50 μM) with AuNPs (1000 μl , 5×10^{-4} μM) for 1 h at 20°C , then centrifuging at 10000 rpm for 5 min to remove the unbound proteins. 50 μl phosphate buffer solution (PBS, 10 mM, pH 7.2) was used to re-suspend the sediment. These steps were repeated three times to wash the conjugates. The samples for field emission TEM (Tecnai G2 G20 S-Twin, FEI, USA) observation were prepared by placing 5 μl of freshly prepared AuNP- β lg conjugates on aluminum stubs covered with a carbon substrate. The stubs were quickly frozen by liquid nitrogen.

2.4. Dynamic light scattering. AuNP- β lg conjugates were prepared by incubating at the molar ratios (β lg: AuNPs) of 100: 1, 500:1, 1000:1, 2000:1, 3000:1, 4000:1, 6000:1, 10000:1 and 30000:1, following the same preparation protocol as for TEM. All the solutions were filtered through a PTFE 0.45 μ m filter. The hydrodynamics diameters of the β lg, AuNPs, and AuNP- β lg conjugates were estimated by an average of three separate measurements by DLS (Nicomp 380, PSS, USA). The data collection time was set to 60 s for temperature equilibrium and 5 s during kinetic series acquisition.

2.5. Isothermal titration calorimetry. All ITC experiments were performed on a MicroCal ITC-200 system (GE Healthcare, USA) and conducted in 10 mM PBS (pH 7.2) at 20 °C. Proteins and AuNP solutions were thoroughly degassed by gentle stirring under vacuum for 5 min before titration. The β lg was titrated into the AuNPs solutions (200 μ l, 5×10^{-4} μ M). The reference cell contained 10 mM PBS (pH 7.2). The injection syringe was filled with 40 μ l of 30 μ M β lg solution. Titration consisted of 20 injections, with 0.5 μ l for the first injection and 2 μ l each subsequent injection. A blank titration of protein into the buffer under the same conditions was performed to determine the mixings and dilutions heats, which were later subtracted from the heat obtained during the titration of protein into the AuNPs suspensions.

2.6. Fluorescence quenching. All protein quenching experiments were performed on a Cary Eclipse fluorescence spectrophotometer (Varian, Sweden). The β lg concentration was 0.01 mM, and the concentration range of AuNPs was from 0 to 5×10^{-4} μ M. The incubating temperature was from 0, 20, 40 and 60 °C. The AuNP-protein conjugates at different temperature were all equilibrated to its corresponding temperature before the experiments. Excitation was performed at 295 nm with a slit width of 5 nm and the emission signal was collected from 300 to 500 nm. The values were calculated as an average of triplicate measurements.

2.7. Surface enhanced raman spectroscopy. In order to monitor the kinetics of Au-S formation, the SERS experiments were performed on a Jobin Yvon XploRA (France). The conjugates were obtained by incubating β lg with AuNPs for 1, 4, 7, 9, and 11 h. The spectra were measured at 532 nm (10 mW) excitation and Rayleigh scattering

light was removed by an edge filter. The collection time was set to 30 s and the emission signal was collected from 200 to 800 cm^{-1} . All SERS spectra were the results of a single 1 s accumulation.

2.8. Fourier transform infrared spectroscopy. The AuNPs- β lg conjugates were prepared by incubating β lg (200 μl , 50 μM) with AuNPs (1000 μl , 5×10^{-4} μM) for 1, 4, 7, 9, 11 h. FTIR spectra were recorded at 20°C on a Bomem MB series FITR Spectrometer (Quebec, Canada) equipped with a dTGS detector and purged constantly with dry air as described by Yu's lab [29,30]. A 128-scan interferogram was collected in single-beam mode with 4 cm^{-1} resolution. The relative secondary structure content was determined from a curve-fitting analysis of the amide I band in the range from 1600-1700 cm^{-1} .

2.9. Allergenic experiments. The IgE capacity of AuNPs- β lg conjugates prepared at different incubation time were determined by an indirect ELISA and inhibition ELISA with minor modifications.¹¹ Microtiter plates polystyrene MaxiSorp 96 U-well (Roskilde, Denmark), were coated with 120 μl /well of 5 $\mu\text{g}/\text{ml}$ AuNPs- β lg conjugates in phosphate buffer solution (PBS, 10 mM, pH 7.2), and incubated overnight. The residual free-binding sites were blocked with 1% fish gelatin and washed by PBS/Tween solution (PBST) for 3 times. 100 μl human serum (1:30 in PBST) was added to the wells, incubated for 2 h at 37 °C and washed 3 times, then 100 μl goat anti-human IgE-HRP (1:200 in PBST) was added and incubated. 100 μl tetramethyl benzidine solution was immediately added to each well after washing. The reaction was ended after an appropriate time (40 - 60 min) by adding 100 μl sulfuric acid (2M). The absorbance was measured at 450 nm using a Bio-Rad Microplate Reader. For inhibition ELISA, Microtiter plates were coated, blocked and washed as the indirect ELISA. 100 μl antisera samples (1:10 diluted by human sera) and AuNPs- β lg conjugates (inhibitors) were mixed and incubated 1 h at 37 °C. The wells were filled with 100 μl of each mixture, and incubated at 2 h 37 °C. The subsequent experimental steps were following the same as for the indirect ELISA. The inhibition rate was calculated using the following equation:

$$\text{Inhibition (\%)} = \left(1 - \frac{B}{B_0}\right) \times 100 \quad (1)$$

Where B and B₀ are the absorbance values of the well with and without the inhibitor, respectively.

3. Results and discussion

3.1. AuNPs-βlg conjugates and molar ratio. TEM and DLS are the most commonly used methods for studying protein corona [3,31]. Typical TEM images and DLS results for βlg, AuNPs and AuNP-βlg conjugates are shown in the Figure 2. It can be deemed that the surface of AuNPs was covered by layers of βlg to form a protein corona (Figure 2B). DLS measurements show that the hydrodynamic diameters of the AuNPs increased dramatically from 36.7 ± 4.2 nm for AuNPs to 56.7 ± 5.1 nm for AuNP-βlg conjugates as a result of protein adsorption (Figure 2C). This increase can only be attributed to the molecules adsorbed and not to NPs aggregation (Figure 2A). The βlg bound layers onto AuNPs were estimated by dividing the corona thickness divided by the βlg diameter and the theoretical maximum number of proteins adsorbed on a single AuNP at 100% surface coverage was based on the minimal cross-sectional area [3,32]. In briefly, the surface area of the particles at half a protein diameter above the particle was divided by the protein cross-sectional area to obtain the stoichiometry of βlg. For instance, the diameter of βlg molecules in neutral condition is about 2.1 ± 0.8 nm (Figure 2C). Thus, considering 4 layers, made of “hard” and “soft” coronas, and about 6.6 × 10³ molecules are theoretically adsorbed on the surface. The hard corona is often referred to as being made of irreversible bound proteins, furthermore, defines the biological identity of NPs and disturbs the bioactivities of adsorbed proteins [33,34].

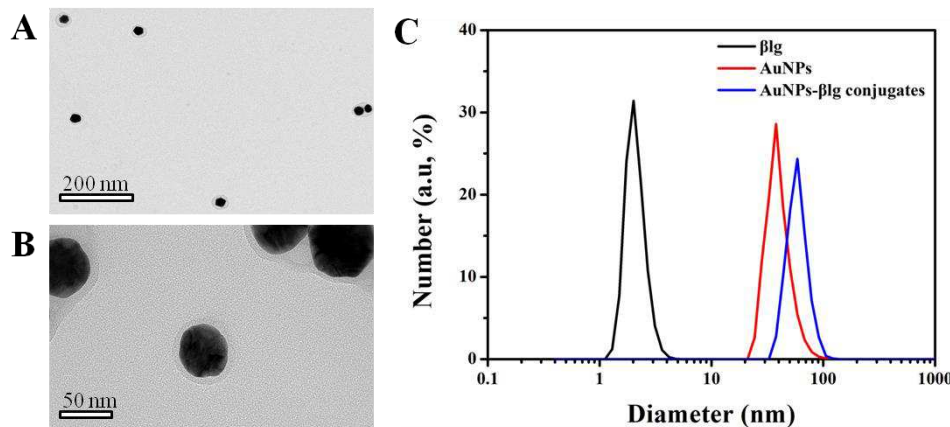


Figure 2. The TEM images (A and B) of AuNPs- β lg conjugates and typical DLS size-distribution for β lg, AuNPs, and AuNPs- β lg conjugates (C).

The hydrodynamic diameter of AuNPs- β lg conjugates as function of different molar β lg/AuNPs ratio from 100 to 30,000 were also obtained by DLS measurements (Figure 3). The results show that the diameter of the conjugates first increases with increasing of β lg concentration, to reach a plateau of \sim 56 nm, when the molar is \sim 4,000. In essence, for the moment, we see there are about 3,600 β lg molecules on a single AuNPs, which indicated the surface coverage was about 55% compared with the theoretical number obtained above. This result is relatively good, since assumptions such as close-packing at the interface and spherical shape of β lg were made in the theoretical calculations.

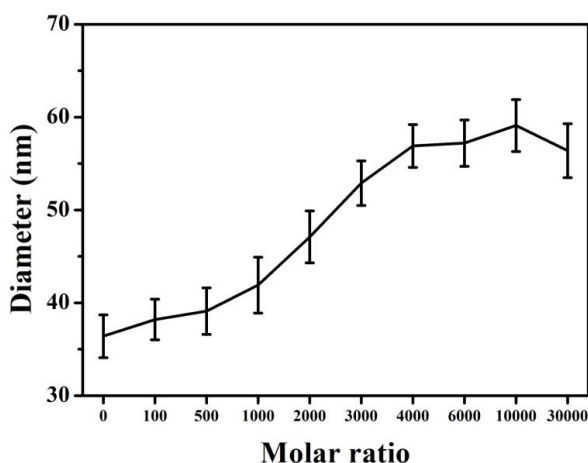


Figure 3. Diameter as a function of AuNPs- β lg conjugates made with molar ratio of β lg/AuNPs. Bars corresponds to standard deviations.

3.2. Detection of K_a and stoichiometry. ITC is a straightforward method for studying the protein-NPs interaction with a high signal-to-noise ratio [35,36]. The

binding parameters of stoichiometry, K_a and enthalpy change (ΔH) can be assessed by monitoring the interaction heat in the sample cells compared to a reference cells [3,32]. The global calorimetry data of ITC were analyzed by the published methods [37,38]. All the ITC curves were collected automatically by Origin software with the subtracted basal heat. The free energy change (ΔG) and entropy change (ΔS) are calculated according to the eqn (2) and (3) below:

$$\Delta G = -RT \ln K_a \quad (2)$$

$$\Delta G = \Delta H - T\Delta S \quad (3)$$

Where K_a is the binding affinity, R is gas constant and T is the absolute temperature.

K_a is one of key factors, which describes the binding behavior of proteins and NPs, and can give a general idea of whether one protein would be replaced by another one [3,39]. β lg (30 μ M) was titrated into 40 nm AuNPs solution (40 nm, 2.5×10^{-4} μ M) to estimate the stoichiometry, K_a , and ΔH of NPs-protein interaction, as exemplified in Figure 4. The area beneath each peak represents the heat exchange within the calorimeter cell containing AuNPs after each injection of β lg [37]. The results show that the negative injection signals implied a strongly exothermic process ($\Delta H < 0$) and the results show a gradually decreased with the increasing of β lg injections due to the reduction of AuNPs remaining in the sample cell. When the molar ratio reached $\sim 7,000$, all of the reactions reached an equilibrium, which suggested that $\sim 3,500$ β lg molecules adsorbed on a single AuNPs molecule (Figure 4A). This value of $\sim 3,500$ is in very good agreement with the results obtained by DLS (Figure 3).

The thermodynamic parameters of stoichiometry, K_a , ΔH and ΔS as a function of the total β lg concentration in the syringe and AuNPs concentration can be derived using nonlinear least-squares fitting (Table 1). The results indicate that β lg association with AuNPs is an entropy-driven process ($\Delta S < 0$) [30]. K_a was measured as being $2.9 \times 10^6 \text{ M}^{-1}$, which is often considered a moderate-strength binding. The thiol groups

contributed to this binding and then defined the change in structure and function of proteins after conjugation with AuNPs [3,40].

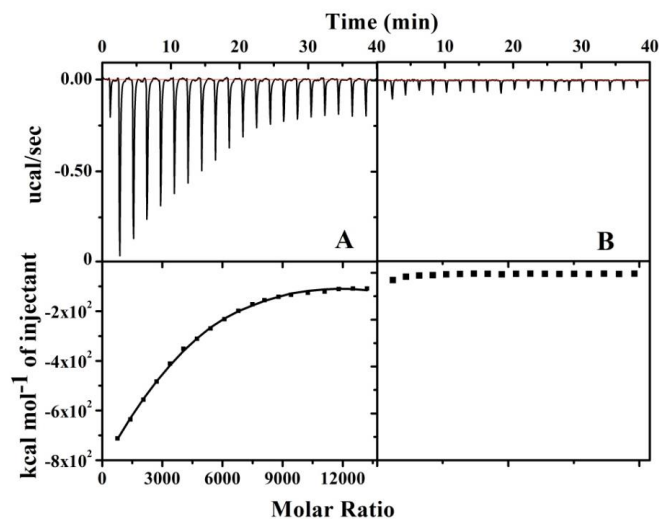


Figure 4 (A) Titration of β lg (30 μ M) was titrated into the AuNPs (5×10^{-4} μ M) at 20 $^{\circ}$ C. Upper figure is the raw data and lower figure represent the integrated heats for each injection plotted against β lg:AuNPs ratio. Solid line is obtained from a one site binding model. (B) β lg (30 μ M) titrated into PBS solution for comparison.

Table 1. Stoichiometry parameter, K_a , ΔH and ΔS as determined by ITC

Temperature	Stoichiometry ^a ($\times 10^3$)	K_a^a ($\times 10^6$ M^{-1})	ΔH ($\times 10^6$ $J M^{-1}$)	ΔG^b ($\times 10^4$ J)	ΔS^b ($\times 10^4$ $J M^{-1} deg^{-1}$)
20 $^{\circ}$ C	3.5 ± 0.5	2.9 ± 0.7	-3.2 ± 1.3	-3.6	-1.1

^aderived from one site binding model, ^bcalculated according to the eqn (2) and (3).

3.3. Detection of K_a by Fluorescence quenching. Fluorescence quenching is an indirect photophysical techniques widely applied in characterizing various aspects of the NPs-protein interaction due to its high sensitivity, convenience and reproducibility [41,42]. Tryptophan, tyrosine and phenylalanine residues have specific fluorescence emission characteristics that are convenient handles when investigating the binding behaviors between proteins and NPs [43]. β lg molecules contains 2 tryptophan, 4 tyrosine and 5 phenylalanine residues, and most of them are located at the surface [44]. When β lg adsorbs on the surface of NPs, these residues would be accessible within quenching distance [40]. The quenching efficiency, described by K_a , depends on the distance between the quencher and the chromophore. K_a is calculated according to eqn (4) [45]:

$$\log[(F_0 - F)/F] = n \log[D] + \log K_a \quad (4)$$

Where F_0 and F are maximum fluorescence intensities of the protein in the absence and presence of quencher, respectively. D is the quencher concentration, and n is the number of binding site of a single molecule.

The adsorption of β lg on the surface of AuNPs occurs mainly due to fast (minutes) electrostatic interaction drawing the chromophore in quenching distance (Figure S1) and a slow formation of covalent bonds in hours that further attach the proteins [11]. The effect of AuNPs on the fluorescence intensity of β lg as function of temperature is illustrated in Figure 5, which shows the emission spectra in the presence and absence (control) of the AuNPs. As expected, AuNPs at 40 nm efficiently quench the β lg fluorescence, and the relative kinetic efficiency of fluorescence quenching can be estimated using Eq. 4 (Figure S2), by calculating K_a and n for different temperatures (Table 2). Notably, the value of K_a at 20 °C ($2.5 \times 10^6 \text{ M}^{-1}$) is in agreement with that derived from ITC measurement ($2.9 \pm 0.7 \times 10^6 \text{ M}^{-1}$). Moreover, K_a decreased with the increase in temperature, indicating weakening of the conjugates at higher temperatures, suggesting static quenching and unfavorable entropy. This results in ground-state complex formation between the fluorophores and NPs. In addition, at all temperatures investigated here, n is approximated to 1, signaling that there is a single binding site on β lg for AuNPs.

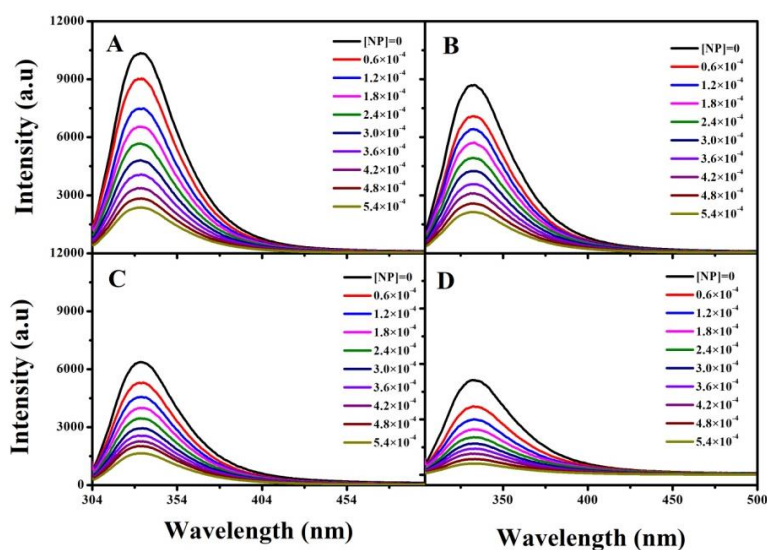


Figure 5 Fluorescence quenching spectra of β lg (0.01 mM) by 40 nm AuNPs (0 to $5.4 \times 10^{-4} \mu\text{M}$) at (A) 0°C, (B) 20 °C, (C) 40°C, and (D) 60°C.

Table 2. The K_a and n of β lg adsorbed on AuNPs at different temperature determined by fluorescence quenching

Temperature	K_a ($\times 10^6$ M ⁻¹)	n^a	R^2 ^b
0 °C	3.1	1.03	0.993
20 °C	2.5	0.97	0.989
40 °C	2.2	1.10	0.994
60 °C	1.8	0.95	0.992

^a n is the number of β lg binding site.

^b R^2 is the correlation coefficient from the least squares fit.

3.4. Detection of Au-S covalent bond. Surface-enhanced raman scattering (SERS) has been proven to be a powerful, ultra-sensitive, and reliable analytical tool for the detection of analytes even at the single-molecule level [46,47]. β lg contains a single cysteine and 2 pairs of disulfide bonds. The thiol group can be easily attached to AuNPs to form the Au-S covalent bond, observed at 296 cm^{-1} by Raman spectroscopy [48].

Covalent bond is the main force involved in the attachment of proteins on the surface of NPs, and this can induce a change in the secondary structure and bioactivity of the protein [14,24]. The SERS spectrum of AuNPs- β lg conjugates as a function of the incubation time is shown in Figure 6. It can be seen that the conjugates exhibit a Raman peak at 296 cm^{-1} , whereas, β lg and AuNPs alone do not show any peak at this shift. The intensity of Au-S bonds peak increases with time to reach a maximum after ~ 9 h incubation, indicating that formation of Au-S bonds takes ~ 9 h in the AuNPs- β lg conjugates, which defined the completely change in the structure and properties β lg.

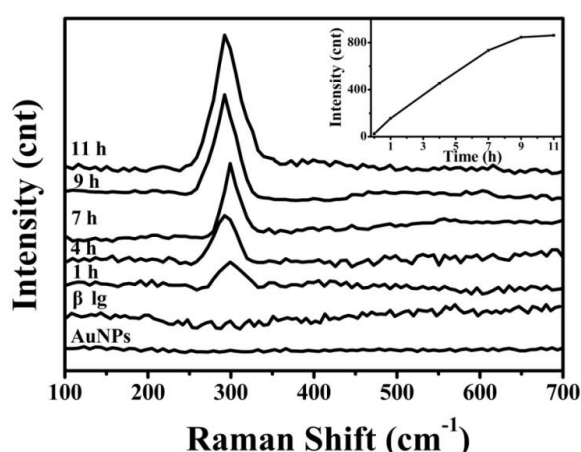


Figure 6 Raman spectra of AuNPs, β lg, and AuNPs- β lg conjugates at different incubation time. Inert, the intensity of AuNPs- β lg conjugates as a function of incubation time.

3.5. Detection of secondary structure. FTIR is a vibrational spectroscopy technique for studying the structure analysis of proteins in aqueous environments [14]. The

second-derivative spectrum of the amide I band ($1700\text{-}1600\text{ cm}^{-1}$) has been widely used to analyze the secondary structure of proteins and polypeptides, and the method is not limited by the protein size or the physical state of the samples [29,30]. FTIR was performed to probe the effect of Au-S interaction on the secondary structures of β lg as a function of time. The fitted inverted second-derivative amide I curves of AuNPs- β lg conjugates at different incubation times are shown in Figure 7 and the resulting secondary structural components are summarized in Table 3. The β -sheet (1628 and 1637 cm^{-1}), the main secondary structural component of β lg (Figure 7A) are is consistent with the results from X-ray crystallography (PDB: 6QPE). The results show that the significant changes in the secondary structure composition of β lg occurred over time after its adsorption on the AuNPs surface. The intensity of bands assigned to β -sheet and 3_{10} -helix (1663 cm^{-1}) decreased, whereas, the bands assigned to α -helix (1658 cm^{-1}), β -turn (1667 and 1675 cm^{-1}) and random coil (1648 cm^{-1}) increased. The spectrum and structural composition do not further change after 9 h incubation (Figure 7E), which is well consistent with the time needed to form Au-S bonds observed by SERS. This result indicates that the formation of Au-S bonds is the main effect inducing the changes in secondary structure changes upon β lg adsorption on AuNPs. The disulfide bridges are located at different place (Figure S3A, Supporting Information), Cys66-Cys160 is likely directly in contact with AuNPs surface, while, Cys106-Cys119 and a free thiol group (Cys121), which are located in the core region of the protein, may require longer time to come into contact with the AuNPs. This may be the reason for the continuous protein structural changes with the incubation time.

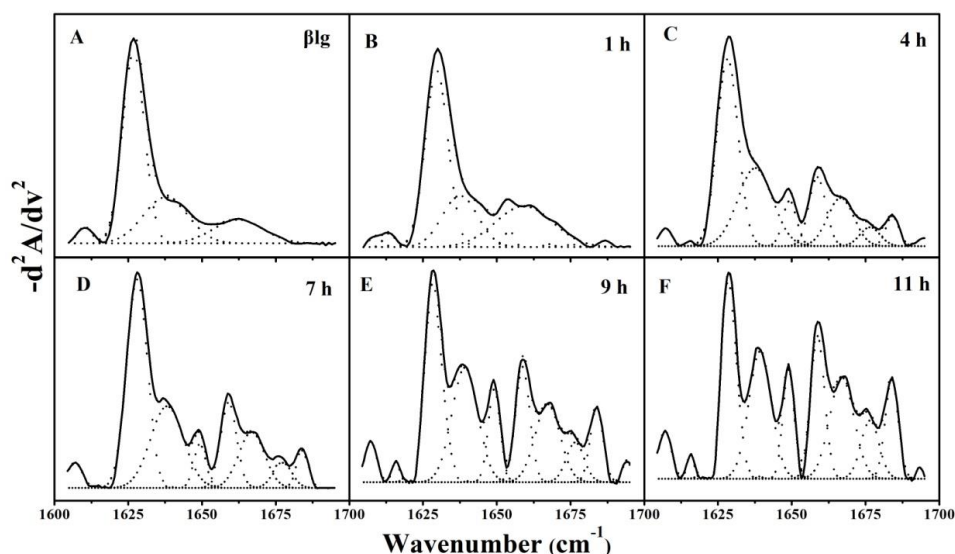


Figure 7 Curve-fitted inverted second-derivative amide I (1600~1700 cm^{-1}) spectrum of βlg adsorbed on 40 nm AuNPs at different incubation times (A) βlg alone, (B) 1 h, (C) 4 h, (D) 7 h, (E) 9 h, (F) 11h.

Table 3. Secondary structural component of βlg adsorbed to AuNPs- βlg conjugates as different incubation time as detected by FTIR.

	3_{10} -helix ^a	α -helix ^b	β -sheet ^c	β -turn ^d	Side chain ^e	Random coil ^f
0	15%	0	81%	0	4%	0
1 h	8%	8%	65%	12%	4%	3%
4 h	0	15%	55%	22%	6%	2%
7 h	0	21%	39%	30%	5%	5%
9 h	0	24%	32%	35%	3%	6%
11 h	0	22%	35%	33%	4%	6%

^a 3_{10} -helix is 1663 cm^{-1} , ^b α -helix is 1658 cm^{-1} , ^c β -sheet is 1628 and 1637 cm^{-1} , ^d β -turn is 1667 and 1675 cm^{-1} , ^eSide chain is 1617 cm^{-1} , ^fRandom coil is 1648 cm^{-1} in the FTIR spectrum [47].

3.6. Inhibition of IgE combining capacity. βlg is the main whey protein and the most frequently and intensively recognized by human IgE, which mediates type I hypersensitivity reactions, including both systemic and localized anaphylaxis [49,50]. The combining capacity of IgE is the main assessment criteria of allergy, and it can be determined by indirect ELISA and inhibition ELISA [51,52].

For protein mixtures, the formation of protein corona is a continuous dynamic exchange process where the proteins with higher K_a would displace at the surface of NPs those with a lower one [11,53]. In order to eliminate the effect of IgE adsorption to AuNPs, and then influence its combining capacity with βlg , the titration of IgE-HRP into AuNPs were also carried out to determine the binding parameters (Figure S4 and Table S1). The results show that the K_a is $1.1 \times 10^6 \text{ M}^{-1}$, which is lower than that of AuNPs- βlg ($2.9 \pm 0.7 \times 10^6 \text{ M}^{-1}$), indicating that the adsorption of

β lg on the surface of AuNPs would not be hindered by the presence of IgE [11]. In addition, we also conjugated β lg with FITC to obtain the β lg-FITC (β lg*) at pH 8 according to our previous work [19], followed by incubation with AuNPs to form AuNPs- β lg* conjugates, then added IgE-HRP to monitor the β lg* fluorescence intensity changes as function of time (Figure S5) [19]. The results show that the intensities were not affected, meaning that the concentration of β lg* did not change, and thus confirmed the adsorbed β lg* would not be replaced by IgE during indirect ELISA and inhibition ELISA experiments [11].

The binding capacity of IgE at different incubation time with AuNPs- β lg conjugates was studied by indirect ELISA and inhibition ELISA (Figure 8). The results show that the IgE combining inhibition increased with the increase of the incubation time. The inhibition reached a maximum at ~9 h, which is consistent with the time required for the complete formation of Au-S bonds and complete change in the secondary structure of the adsorbed β lg (Figure 7). This time point indicates that the IgE combining capacity changes is related to the structural changes of β lg. There are three main IgE allergenic epitopes located at 41-60, 102-124, 149-162 in its amino acids sequence, and most are assigned β -sheet [54]. The three dimensional model (Fig. S3B) indicates that these three epitopes are stabilized by a ring formed by disulfide or hydrogen bonds. The reaction of β lg and AuNPs needs to break the disulfide bonds of β lg firstly, then form an Au-S bond, which would destroy the structure of these epitopes and their anaphylaxis (IgE binding capacity). Furthermore, the FTIR confirmed a decrease of β -sheet contents of β lg molecule after conjugated with AuNPs, indicating the conformation change of the three main IgE allergenic epitopes.

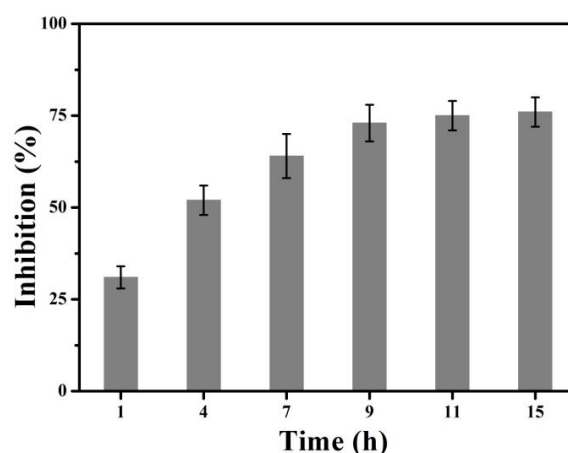


Figure 8 The changes of IgE binding abilities of AuNPs-βlg conjugates at different incubation time as determined by inhibition ELISA.

4. Conclusion

Proteins, especially βlg, adsorb on the surface of AuNPs to form the protein corona (AuNPs-βlg conjugates) when it exposed to milk. This adsorption results mainly from a fast electrostatic force (minutes) and a slow formation of Au-S covalent bonds (hours). The protein corona may have many effects on living organisms, on one hand, it dominates the cellular uptake and intracellular fate of NPs in living systems, and on the other hand, it induces changes in structure and conformation of adsorbed proteins, their bioactivities and functions. The allergenicity of βlg would change after conjugated with AuNPs.

In summary, the binding mechanism is the key to study the bioapplication of NPs. The binding parameters, namely, stoichiometry, K_a and time evolution of Au-S bond and general secondary structure changes were assessed to address the desensitization mechanism. The results showed that about 3,600 βlg molecules are adsorbed on a single AuNPs and the K_a is $2.9 \pm 0.7 \times 10^6 \text{ M}^{-1}$, indicating a moderate-strength interaction. The formation of Au-S bonds takes ~9 h, which is the time needed for complete changes in the secondary structure and in IgE combining capacity. The structure and conformation of allergenic epitopes were destroyed by the formation of Au-S bond, then induced to the decrease of allergy.

Supporting information

Supporting Information is available from the Wiley Online Library or from the author.

Acknowledgements

The authors would like to thank Prof. Shaoning Yu for assistance with the detection of secondary structure.

Authors' contributions

ZXN performed the experimental work and contributed to the analysis and representation of data. The manuscript was written by CZ. LMF, SXL, HY performed parts of experiments. ZXN, LYP, ZXZ and HXW contributed to the experimental design. All authors were involved in writing the manuscript. All authors read and approved the final manuscript.

Funding

This work was supported by National Natural Science Foundation of China (No. 31470786 and 81871690), and Science and Technology Commission of Shanghai (No.19441903800).

Availability of data and materials

The datasets used and/or analyzed during the current study are available from the corresponding author on reasonable request.

Ethics approval and consent to participate

No applicable.

Competing interests

The authors declare that they have no competing interests.

Author details

¹School of Food Science & Engineering, Qilu University of Technology, Jinan 250353, China

²School of public health, Chengdu University of traditional Chinese medicine, Chengdu 610075, China

³College of Biomass Sciences and Engineering, Sichuan University, Chengdu 610065, China

⁴State Key Laboratory of Biobased Materials and Green Papermaking, Qilu University of Technology, Jinan 250353, China

REFERENCE

1. Krawinkel J, Richter U, Torres-Mapa M L, et al. Optical and electron microscopy study of laser-based intracellular molecule delivery using peptide-conjugated photodispersible gold nanoparticle agglomerates. *J. nanobiotechnol.*, 2016, 14(1): 2.
2. Fahimi-Kashani N, Hormozi-Nezhad M, Gold-nanoparticle-based colorimetric sensor array for discrimination of organophosphate pesticides. *Anal. Chem.*, 2016, 88, 8099-8106.
3. Zhang X, Zhang J, Zhang F, Yu S. Probing the binding affinity of plasma proteins adsorbed on Au nanoparticles. *Nanoscale*. 2017, 9, 4787-4792.
4. Cui M, Liu R, Deng Z. et al. Quantitative study of protein coronas on gold nanoparticles with different surface modifications. *Nano Res.*, 2014, 7(3), 345-352.
5. Ammar A, Sierra D, Mérola F, Hildebrandt N, Guével, X. Self-assembled gold nanoclusters for bright fluorescence imaging and enhanced drug delivery. *ACS Nano*, 2016, 10(2), 2591-2599.
6. Chien C C, Chen H H, Lai S F, Wu K C, Cai X, Hu Y, et al. Gold nanoparticles as high-resolution X-ray imaging contrast agents for the analysis of tumor-related micro-vasculature. *J. Nanobiotechnol.*, 2012, 10(1), 10.
7. Ma Q, Wang Y, Jia J, Xiang Y, Colorimetric aptasensors for determination of tobramycin in milk and chicken eggs based on DNA and gold Nanoparticles. *Food Chem.*, 2018, 249, 98-103.
8. Li L, Li B, Cheng D, Mao L. Visual detection of melamine in raw milk using gold nanoparticles as colorimetric probe. *Food Chem.*, 2010, 122(3), 895-900.
9. Müller L, Simon J, Rosenauer C, et al. The transferability from animal models to humans: challenges regarding aggregation and protein corona formation of nanoparticles. *Biomacromolecules*, 2018, 19(2), 374-385.
10. Cedervall T, Lynch I, Lindman S, Berggård T, Thulin E, Nilsson H, Dawson K, Linse S. Understanding the nanoparticle-protein corona using methods to quantify exchange rates and affinities of proteins for nanoparticles. *Proc. Natl. Acad. Sci. U.S.A.* 2007, 104(7), 2050-2055.
11. Zhang X, Shi H, Zhang R, Zhang J, Xu F, Qiao L, Yu S. The competitive dynamic binding of some blood proteins adsorbed on gold nanoparticles. *Part. Part. Syst. Char.*, 2018, 36(1), 1800257.

12. Chanana M, Rivera G, Correa M, Liz-Marzán L, Parak W. Physicochemical properties of protein-coated gold nanoparticles in biological fluids and cells before and after proteolytic digestion. *Angew. Chem. Int. Edit.*, 2013, 52(15), 4179-4183.
13. Gunawan C, Lim M, Marquis C, Amal, R. Nanoparticle-protein corona complexes govern the biological fates and functions of nanoparticles. *J. Mater. Chem. B* 2014, 2(15), 2060-2083.
14. Carril M, Padro D, Pino P, Carrillo C, Gallego M, Parak W. In situ detection of the protein corona in complex environments. *Nat. Commu.*, 2017, 8(1), 1542-1547.
15. Wang M, Fu C, Liu X, Lin Z, Yang N, Yu S. Probing the mechanism of plasma protein adsorption on Au and Ag nanoparticles with FT-IR spectroscopy. *Nanoscale*, 2015, 7(37), 15191-1596.
16. Visalakshan R., MacGregor M, Sasidharan S, Ghazaryan A, et al. Biomaterial surface hydrophobicity-mediated serum protein adsorption and immune responses. *ACS Appl. Mater. Inter.*, 2019, 11(31), 27615-27623.
17. Bunyavanich S, Shen N, Grishin A, Wood R, Burks W, Dawson P. Early-life gut microbiome composition and milk allergy resolution. *J. Allergy Clin. Immunol.*, 2016, 138(4), 1122-1130.
18. Canani R, Sangwan N, Stefka A, Nocerino R, Paparo L, Aitoro, R. Lactobacillus rhamnosus GG-supplemented formula expands nutyrate-producing bacterial strains in food allergic infants. *ISME J.*, 2016, 10(3), 742-750.
19. Zhang X, Hemar Y, Lv L, Zhao T, Yang Y, Han Z. Molecular characterization of the β -lactoglobulin conjugated with fluorescein isothiocyanate: binding sites and structure changes as function of pH. *Int. J. Biol. Macromol.*, 2019, 140, 377-383.
20. Guo Y, Harris P, Kaur A, Pastrana L, Jauregi P. Characterisation of β -lactoglobulin nanoparticles and their binding to caffeine. *Food Hydrocolloid*, 2017, 71, 85-93.
21. Kurpiewska K, Biela A, Loch J, Lipowska J, Siuda M, Lewiński K. Towards understanding the effect of high pressure on food protein allergenicity: β -lactoglobulin structural studies. *Food Chem.*, 2019, 270, 315-321.
22. Sari T P, Mann B, Kumar R, Singh R R., Sharma R, Bhardwaj M, Athira S. Preparation and characterization of nanoemulsion encapsulating curcumin. *Food Hydrocolloids*, 2015, 43, 540-546.

23. Corzo-Martínez M, Moreno F J, Villamiel M, Patino J, Sánchez C C. Effect of glycation and limited hydrolysis on interfacial and foaming properties of bovine β -lactoglobulin. *Food hydrocolloids*, 2017, 66, 16-26.
24. Fu C, Yang H, Wang M, Xiong H, Yu S. Serum albumin adsorbed on Au nanoparticles: structural changes over time induced by S-Au interaction. *Chem. Commun.*, 2015, 51(17), 3634-3636.
25. Liu L, Zeng L, Wu L, Jiang X. Revealing the effect of protein weak adsorption to nanoparticles on the interaction between the desorbed protein and its binding partner by surface-enhanced infrared spectroelectro chemistry. *Anal. Chem.*, 2017, 89(5), 2724-2730.
26. Wei S, Ahlstrom L, Brooks C. Exploring protein-nanoparticle interactions with coarse-grained protein folding models. *Small*, 2017, 13(18), 1603748.
27. Frens G. Controlled nucleation for the regulation of the particle size in monodisperse gold suspensions. *Nat. Phys. Sci.*, 1973, 241(15), 20-22.
28. Haiss W, Thanh N, Aveyard J, Fernig D. Determination of size and concentration of gold nanoparticles from UV-Vis spectra. *Anal. Chem.*, 2007, 79(11), 4215-4221.
29. Yang H, Yang S, Kong J, Dong A, Yu S. Obtaining information about protein secondary structures in aqueous solution using fourier transform IR spectroscopy. *Nat. protoc.*, 2015, 10(3), 382.
30. Kong J, Yu S. Fourier transform infrared spectroscopic analysis of protein secondary structures. *Acta Bioch. Bioph. Sin.*, 2007, 39(8), 549-559.
31. Tenzer S, Docter D, Kuharev J, Musyanovych A, Fetz V, Hecht R. Rapid formation of plasma protein corona critically affects nanoparticle pathophysiology. *Nat. Nanotechnol.*, 2013, 8(10), 772.
32. Lindman S, Lynch I, Thulin E, Nilsson H, Dawson K, Linse S. Systematic investigation of the thermodynamics of HSA adsorption to N-iso-propylacrylamide/N-tert-butylacrylamide copolymer nanoparticles. Effects of particle size and hydrophobicity. *Nano Lett.*, 2007, 7(4), 914-920.
33. Milani S, Baldelli B, Pitek A, Dawson K, Radler J. Reversible versus irreversible binding of transferrin to polystyrene nanoparticles: soft and hard corona. *ACS Nano*, 2012, 6(3), 2532-2541.

34. Kelly P, Åberg C, Polo E, O'connell A, Cookman J, Fallon J. Mapping protein binding sites on the biomolecular corona of nanoparticles. *Nat. Nanotechnol.*, 2015, 10(5), 472-479.
35. Schöttler S, Landfester K, Mailänder V. Controlling the stealth effect of nanocarriers through understanding the protein corona. *Angew. Chem. Int. Edit*, 2016, 55, 8806-8815.
36. Velazquez A, Freire E. Isothermal titration calorimetry to determine association constants for high-affinity ligands. *Nat. Protoc.*, 2006, 1(1), 186-191.
37. Brautigam C, Zhao H, Vargas C, Keller S, Schuck P. Integration and global analysis of isothermal titration calorimetry data for studying macromolecular interactions. *Nat. Protoc.*, 2016, 11(5), 882.
38. Li F, Yu T, Yu S. Structural dynamic and thermodynamic analysis of calcineurin B subunit induced by calcium/magnesium binding. *Int. J. Biol. Macromol.*, 2013, 60, 122-127.
39. Vilanova O, Mittag J, Kelly P, Milani S, Dawson K, Rädler J. Understanding the kinetics of protein-nanoparticle corona formation. *ACS Nano*, 2016, 10(12), 10842-1850.
40. Creutz S, Peters J. Exploring secondary-sphere interactions in Fe-N_xH_y complexes relevant to N₂ fixation. *Chem. Sci.*, 2017, 8(3), 2321-2328.
41. Lacerda S, Park J, Meuse C, Pristinski D, Becker M, Karim A, Douglas J. Interaction of gold nanoparticles with common human blood proteins. *ACS Nano*, 2010, 4(1), 365-379.
42. Pezzato C, Maiti S, Chen J, Cazzolaro A, Gobbo C, Prins L. Monolayer protected gold nanoparticles with metal-ion binding sites: functional systems for chemosensing applications. *Chem. Commun.*, 2015, 51(49), 9922-9931.
43. Zou Q, Liu K, Abbas M, Yan X. Peptide-modulated self-assembly of chromophores toward biomimetic light-harvesting nanoarchitectonics. *Adv. Mater.*, 2016, 28(6), 1031-1043.
44. Ueno H, Kato T, Ohnishi H, Kawamoto N, Kato Z, Kaneko H. T-cell epitope-containing hypoallergenic β -lactoglobulin for oral immunotherapy in milk allergy. *Pedia. Allergy Immu.*, 2016, 27(8), 818-824.
45. Peng X, Wang X, Qi W, Su R, He Z. Affinity of rosmarinic acid to human serum albumin and its effect on protein conformation stability. *Food chem.*, 2016, 192, 178-187.
46. Reguera J, Langer J, Aberasturi D, Liz-Marzán L. Anisotropic metal nanoparticles for surface enhanced raman scattering. *Chem. Soc. Rev.*, 2017, 46(13), 3866-3885.

47. Hu Y, Cheng H, Zhao X, Wu J, Muhammad F, Lin S. Surface-enhanced raman scattering active Gold nanoparticles with enzyme-mimicking activities for measuring glucose and lactate in living tissues. *ACS Nano*, 2017, 11(6), 5558-5566.
48. Zhang D, Neumann O, Wang H, Yuwono V, Barhoumi A, Perham M. Gold nanoparticles can induce the formation of protein-based aggregates at physiological pH. *Nano Lett.*, 2009, 9(2), 666-671.
49. Wu X, Lu Y, Xu H, Lin D, He Z, Wu H. Reducing the allergenic capacity of β -lactoglobulin by covalent conjugation with dietary polyphenols. *Food Chem.*, 2018, 256, 427-434.
50. Villas-Boas M, Benedé S, Lima R, Netto F, Molina E. Epitopes resistance to the simulated gastrointestinal digestion of β -lactoglobulin submitted to two-step enzymatic modification. *Food Res. Int.*, 2015, 72, 191-197.
51. Foegeding E A, Plundrich N, Schneider M, Campbell C, Lila M A. Protein-polyphenol particles for delivering structural and health functionality. *Food hydrocolloids*, 2017, 72, 163-173.
52. Wei T, Du D, Zhu M, Lin Y, Dai Z. An improved ultrasensitive enzyme-linked immunosorbent assay using hydrangea-like antibody-enzyme-inorganic three-in-one nanocomposites. *ACS Appl. Mater. Inter.*, 2016, 8(10), 6329-6335.
53. Cedervall T, Lynch I, Foy M, Berggård T, Donnelly S, Cagney G. Detailed identification of plasma proteins adsorbed on copolymer nanoparticles. *Angew. Chem.Int. Edit.*, 2007, 46(30), 5754-5756.
54. Hartmann R, Wal J, Bernard H, Pentzien A. Cytotoxic and allergenic potential of bioactive proteins and peptides. *Curr. Pharm. Design*, 2007,13(9), 897-920.

Supplementary Files

This is a list of supplementary files associated with this preprint. Click to download.

- [Supportinginformation.docx](#)